Experimental and theoretical study of the $^2\mathrm{H}(\vec{d},\gamma)^4\mathrm{He}$ reaction below $E_{\mathrm{c.m.}}=60$ keV

K. Sabourov, M. W. Ahmed, S. R. Canon, B. Crowley, K. Joshi, J. H. Kelley, S. O. Nelson, B. A. Perdue, E. C. Schreiber, A. Sabourov, A. Tonchev, H. R. Weller, and E. A. Wulf
Department of Physics, Duke University, Durham, North Carolina 27708, USA and Triangle Universities Nuclear Laboratory, Box 90308, Durham, North Carolina 27708, USA

R. M. Prior and M. C. Spraker
Department of Physics, North Georgia College and State University, Dahlonega, Georgia, 30597, USA

H. M. Hofmann and M. Trini
Physics Department, University of Erlangen-Nürnberg, Erlangen, Germany
(Received 14 May 2004; published 1 December 2004)

New measurements of the analyzing powers A_y and T_{20} have been obtained for the $^2\mathrm{H}(d,\gamma)^4\mathrm{He}$ reaction at a laboratory beam energy of 115 keV. A transition matrix element analysis results in a unique solution which indicates that the reaction proceeds by 55% $E2$, 29% $E1$, and 16% $M2$ radiation. These results are shown to be in good agreement with the results of a new refined resonating group model calculation. The impact of these results on the extrapolated value of the astrophysical S factor for this reaction is discussed.

DOI: 10.1103/PhysRevC.70.064601 PACS number(s): 25.40.Lw, 24.70.+s, 26.35.+c, 24.10.Eq

I. INTRODUCTION

The deuteron-deuteron radiative capture reaction is one of the deuterium burning processes for which the cross section at very low energies, and therefore the astrophysical S factor, is not very well known. The "traditional" value of the S factor for this reaction at zero energy proposed by Fowler, Caughlan, and Zimmerman [1] was subsequently increased by a factor of about 30 by Assenbaum and Langanke [2]. This work was motivated by tensor polarized studies of the d+d capture reaction at energies of several to 50 MeV [3–7] which firmly established the presence of a D-state component in the ground state of ^{4}He. The existence of this D-state component made s-wave capture to the ground state of ^{4}He via $E2$ radiation possible and in fact quite dominant at very low energies, which led to the significant enhancement in the extrapolated value of the S factor.

This view (the predominance of s-wave capture to the D state) of the low energy nature of the $^2\mathrm{H}(\vec{d},\gamma)^4\mathrm{He}$ reaction was challenged by low energy studies of the capture reaction with polarized beams [8]. In this work, measurements of A_{yy} and A_y at an incident energy of 80 keV were used to show that 50% or more of the capture strength was due to p-wave capture in the form of either $E1$ or $M2$ radiation. Unfortunately, the data were not able to distinguish between three different solutions which gave a p-wave strength ranging from 50% to 85%, and an $E1/M2$ ratio ranging from 2 to 0.2. At the time, and with these large uncertainties, a satisfactory theoretical explanation of these results was not available.

The $^2\mathrm{H}(\vec{d},\gamma)^4\mathrm{He}$ reaction has unique features as a result of the fact that there are identical bosons in the entrance channel. This requires that the sum of the relative orbital angular momentum and the total spin in the entrance channels be an even number ($l+s$ must be even). This condition restricts the number of partial waves which must be considered. Of course, the low energy severely limits the number of partial waves as a result of barrier penetration considerations. The dominant strength would be expected to be s-wave capture. This will lead to $E2$ radiation going to the D-state component of the ground state and we label this as the $^5s_2$ ($E2$) transition amplitude ($^{2s+1}l_j$). The next transition strength we would expect would be due to p-wave capture. This could result in either $E1$ or $M2$ radiation [$^3p_1$ ($E1$) and $^3p_2$ ($M2$), respectively]. Note that the $E1$ radiation would be isoscalar $\Delta S=1$, leading to both the S and D states of the ground state of ^{4}He. Beyond this, d-wave $E2$ capture to the S state of ^{4}He could also contribute, but it will be seen that the data (and theory) indicate a negligible contribution of this term to the cross section at the energy of this experiment (a beam energy of $E_{\mathrm{c.m.}}=58$ keV).

The intent of the present experimental investigation was to attempt to uniquely determine the amplitudes and phases of the contributing transition matrix elements, with the hopes that this would lead to a deeper understanding and eventually stimulate a quantitative theoretical explanation of the nature of this reaction at these very low energies. As will be shown below, we have been successful in both regards.

II. EXPERIMENT

The vector and tensor analyzing powers for the $^2\mathrm{H}(\vec{d},\gamma)^4\mathrm{He}$ reaction were measured using a tensor-polarized deuteron beam from the atomic beam polarized ion source (ABPIS) at TUNL. The 80-keV deuterons were accelerated to 115 keV by biasing the target chamber. The target consisted of heavy water which was evaporated onto a liquid nitrogen cooled Cu disk inside of the target chamber. The thickness of this ice layer was measured to be more than an order of magnitude greater than that required to completely stop the beam. The protons produced via the $^2\mathrm{H}(d,p)^3\mathrm{H}$ re-

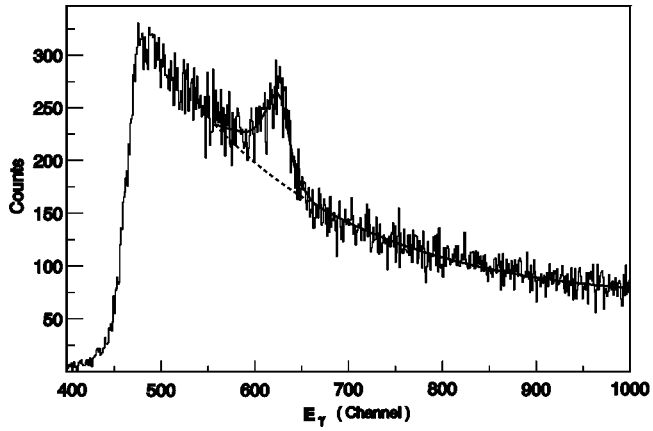

FIG. 1. Energy spectrum produced by a shielded NaI(Tl) detector. The spectrum is a sum of the detector response to the 23.8 MeV capture γ rays, along with the cosmic-ray and neutron induced background. The solid line illustrates the fit used to extract the yield of the 23.8 MeV γ rays from the spectrum, while the dashed line represents the background.

action were detected using a silicon solid-state detector, and used to monitor the condition of the target. A fresh layer of ice was created as soon as any sign of target contamination or deterioration was observed, typically every 4 to 6 h.

The capture γ rays were observed by two shielded $10'' \times 10''$ NaI(Tl) detectors. Passive shielding and plastic anticoincidence shields [9] were used to reduce the neutron and cosmic-ray induced background. A typical resulting spectrum is shown in Fig. 1.

The differential cross section for a reaction initiated by a beam with tensor components t_{kq} is given by

$$\sigma = \sigma_0 \sum_{k,q} t_{kq} T^{*}_{kq}, \tag{1}$$

where σ_0 is the cross section for the unpolarized beam and T_{kq} are the tensor analyzing powers. The beam polarization and the analyzing powers can be written as spherical or as Cartesian tensors, and the tensors are typically considered with respect to the Madison Convention coordinate system [10]. It is convenient to express the beam polarization in terms of the "internal" polarization moments p_ζ and $p_{\zeta\zeta}$ related to the projectile spin-state occupation numbers, and the direction of the spin-symmetry axis with respect to the scattering plane.

For the A_y measurements of this work we used a pure vector-polarized deuteron beam with the spin-symmetry axis set vertically. In this case the yield observed with a detector positioned at angle θ is

$$Y(\theta) = Y_0(\theta)\left(1 + \frac{3}{2} p_\zeta A_y(\theta)\right) \tag{2}$$

where $Y_0(\theta)$ is the yield with the unpolarized beam. By using two polarization states, we can express the A_y analyzing power as an asymmetry

$$A_y(\theta) = \frac{2}{3} \frac{Y_1(\theta) - Y_2(\theta)}{Y_2(\theta) p_{\zeta 1} - Y_1(\theta) p_{\zeta 2}}. \tag{3}$$

In our case the beam was switched between states of $p_\zeta = +0.53$ and $p_\zeta = -0.53$.

For the T_{20} measurements the spin-symmetry axis was set along the beam momentum, i.e., $\beta = 0°$ and $\phi = 0°$. The expression for the yield is

$$Y(\theta) = Y_0(\theta)\left(1 + \frac{1}{\sqrt{2}} p_{\zeta\zeta} T_{20}(\theta)\right). \tag{4}$$

If two states of $p_{\zeta\zeta}$ are used, the resulting expression for the tensor analyzing power is

$$T_{20}(\theta) = \sqrt{2} \frac{Y_1(\theta) - Y_2(\theta)}{Y_2(\theta) p_{\zeta\zeta 1} - Y_1(\theta) p_{\zeta\zeta 2}}. \tag{5}$$

The beam polarization was set to switch between $p_{\zeta\zeta} = +0.80$ and $p_{\zeta\zeta} = -0.80$.

The polarization values were determined by the spin filter polarimeter, and checked with a nuclear polarimeter located in the beam line 2 m in front of the target chamber. This polarimeter utilized the known analyzing powers of the $^2\mathrm{H}(\vec{d},p)^3\mathrm{H}$ reaction, and protons were detected using two silicon surface barrier detectors located on opposite sides of the beamline. The values of p_ζ and $p_{\zeta\zeta}$ were measured both ways and determined to have 5% uncertainties. The polarization states were switched at a frequency of 10 Hz. Data taking was stopped for a period of 7 ms following each switch to avoid any beams of uncertain polarization.

The final spectra were fitted with a function describing the background and the previously determined detector response function [11]. The background was found to be well described using an exponential function with an argument quadratic in energy. Care was taken to use the same background in the two different spin-state spectra since the background displayed no analyzing power. The areas of the fitted response function were used as the γ-ray yields. A typical spectrum and fit are displayed in Fig. 1. The resulting yields were then inserted into Eqs. (3) and (5) to produce the final analyzing powers. The resulting data points are displayed in Fig. 2, along with the previously measured unpolarized cross section data at $E_d = 80$ keV. The data points were corrected for finite geometry effects, which gave corrections of 10% or less.

III. DETERMINATION OF THE TRANSITION MATRIX ELEMENTS

The formalism of Ref. [12] makes is possible to express the observables [$\sigma(\theta)$, $A_y(\theta)$, and $T_{20}(\theta)$] in terms of the amplitudes and the two relative phases of the three transition matrix elements [$^5s_2(E2)$, $^3p_1(E1)$, and $^3p_2(M2)$] expected to be present.

The observed angular distributions of the unpolarized cross section at an effective energy (defined to be the energy at which half of the yield is due to lower energies) of $E_{\mathrm{c.m.}} = 33$ keV [8], and the present analyzing powers A_y and T_{20}, were simultaneously fitted to determine the TME ampli-

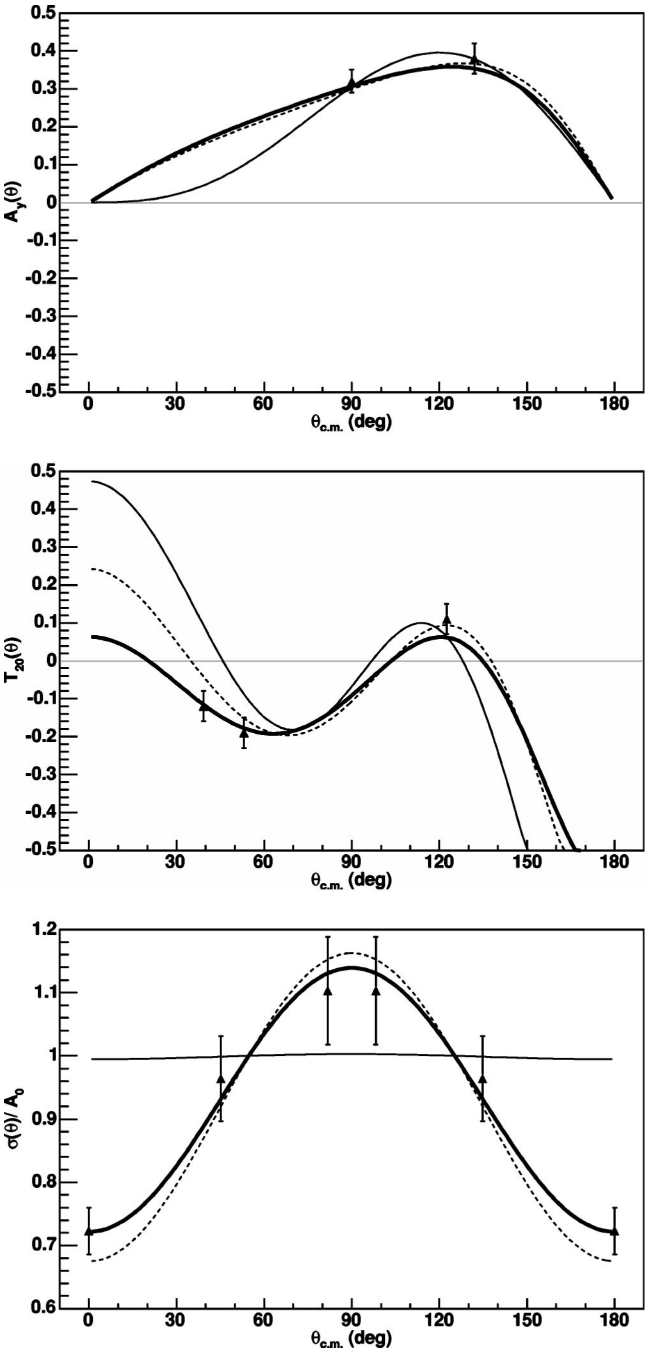

FIG. 2. The $A_y(\theta)$ and $T_{20}(\theta)$ data obtained in the present work are shown along with the previous $\sigma(\theta)/A_0$ data of Ref. [6]. The data points have been corrected for finite geometry effects. The error bars represent the statistical uncertainties, as well as spectra fitting errors and uncertainties in the beam polarization values. The thick lines are the result of a fit to the three transition matrix elements described in the text (see Table I). The thin solid lines are the polarization observables produced by the refined resonating group model calculation, thin dashed lines represent the same calculation with the transition matrix element (TME) phase difference set to the results of TME analysis (see Sec. IV for details).

tudes and relative phases. The use of the lower energy cross section angular distribution was necessary since this was not measured in the present work. This, of course, assumes that this quantity does not change significantly in the energy region between 33 and 46 keV, the effective center-of-mass energies of the previous and present measurements. This assumption is supported by the present theoretical calculations (see Sec. IV) which indicate that this angular distribution is essentially constant in this energy region. The results of the fit are shown along with the data in Fig. 2 and Table I. We note here that if the previously measured unpolarized cross section data are not included in the fitting procedure, the solution obtained agrees with the result presented in Table I, although there is a significant increase in the errors. A search for more solutions was performed by changing the initial values of various parameters. For the amplitudes, the strength of one transition was varied with 20% steps, while all the other amplitudes were held unchanged. For the relative phases, a similar search was performed with 30° steps. The solution presented above was the only solution having χ_v^2 close to unity. This fit produced $\chi_v^2=1.2$, while the next "best" solutions were characterized by χ_v^2 values of 8.8 and 17.3. The results of this search led to the conclusion that the solution of Table I was a unique solution.

We also investigated the possibility of including different sets of matrix elements to accommodate our data. Exclusion of the p waves ($E1$, or $M2$, or both) did not produce satisfactory fits. Inclusion of a d-wave amplitude [the $^1d_2(E2)$ transition being the most logical one, dominating at energies above 1 MeV] resulted in solutions with a negligibly small $^1d_2$ component (below 3% of the total strength) and the same angular dependence for the analyzing powers. This indicated that the choice of matrix elements included in the above analysis provides an adequate representation of the reaction at low energies.

IV. THE REFINED RESONATING GROUP MODEL CALCULATION

We use the refined resonating group model (RRGM) [13–15] to compute the scattering in the ^{4}He system using the Kohn-Hulthén variational principle [16]. The main technical problem is the evaluation of the many-body matrix elements in coordinate space. The restriction to a Gaussian basis for the radial dependencies of the wave function allows for a fast and efficient calculation of the individual matrix elements [13,15]. However, to use these techniques the potentials must also be given in terms of Gaussians. In this work we use suitably parametrized versions of the AV18 [17] NN potential and the UIX [18] three-body force.

In the ^{4}He system we use a model space with six two-fragment channels, namely, the p-^{3}H, the n-^{3}He, the d-^{2}H, the d-^{2}H$(S=0)$, the $\bar{d}$ resonance, the $\bar{d}$-$\bar{d}$, and the (pp)-(nn) channels. The last three are an approximation to the three- and four-body breakup channels that cannot in practice be treated within the RRGM. The ^{4}He is treated as four clusters in the framework of the RRGM to allow for the required internal orbital angular momenta of ^{3}H, ^{3}He, or ^{2}H.

For the scattering calculation we include all s-, p-, and d-wave contributions to the $J^\pi=0^+,1^+,2^+,0^-,1^-$, and 2^- channels. From the R-matrix analysis these channels are known to reproduce the low-energy experimental data. The

TABLE I. Results of the TME fit analysis and refined resonating group model (RRGM) calculations for effective $E_{\mathrm{c.m.}}=46$ keV. The column labeled Strength (%) represents the percent contribution of each TME to the angle integrated cross section.

TME	Multipolarity	TME Fit		RRGM	
	$p\mathcal{L}$	Strength (%)	Phase (deg)	Strength (%)	Phase (deg)
$^5s_2$	$E2$	55 ± 8	0.0	51	0
$^3p_1$	$E1$	29 ± 6	77 ± 3	26	98
$^3p_2$	$M2$	16 ± 3	44 ± 8	23	28

full wave function for these channels contains over 100 different spin and orbital angular momentum configurations; hence it is too complicated to be given in detail. The RRGM can be considered as a kind of variational calculation; hence, increasing the model space used usually improves the calculation. Using a generic algorithm [19] for AV18 and UIX together and allowing for *s*, *p*, and *d* waves on all internal coordinates, we found a triton binding energy of −8.460 MeV for dimension 70. This practically converged result compares favorably with the numerically exact one of Nogga [20] of −8.478 MeV. For the deuteron we used five width parameters for the *s* wave and three for the *d* wave, yielding −2.213 MeV, just 10 keV short of the experimental value. These binding energies yield relative thresholds which reproduce the experimental binding energies and thresholds very well.

This representation of ^{3}H/^{3}He, deuteron, and the unbound *NN* systems forms the model space of the ^{4}He scattering system. We get for the different J^π values five to ten physical channels, insufficient to find reasonable results. So-called distortion or pseudo-inelastic channels [15] without an asymptotic part have to be added to improve the description of the wave function within the interaction region. For this purpose all the configurations calculated for the physical channels but one per channel can be reused, keeping only those width parameters which describe the internal region.

We use the full scattering wave functions in calculating the electromagnetic transition matrix elements, including distortion channels and the 0^+ wave function, omitting the small width parameters as an approximation for the ^{4}He bound-state wave function. The calculated binding energy of ^{4}He is −28.328 MeV. The transition matrix elements are calculated in the long-wavelength limit using Siegert's theorem; for details of the method see Ref. [21]. The amplitude and phases of the contributing TMEs are given in Table I. The agreement is quite good, especially for the relative strengths of the $E2$, $E1$, and $M2$ terms. The observables are plotted and compared to the experimental results in Fig. 2, where the thin lines are the result of the RRGM calculation. While the polarization observables are in reasonable agreement with the data, the angular distribution of the cross section is predicted to be isotropic, in contrast to the data. This discrepancy was found to be due to the difference between the fitted and calculated values of the $E1-M2$ phase difference (33° vs 70°), given in Table I. If the calculated phase difference is set to be equal to 33°, the angular distribution is found to agree much better with the experimental value. This is illustrated by the thin dashed line in Fig. 2. We note that this change of phase has only a very minor effect on the polarization observables.

It is also interesting to compare the solution presented in Table I to the three solutions presented in Ref. 8. In doing so, one finds that the present solution does not agree with any of the solutions presented in Ref. 8, although it does indicate 50% *p*-wave capture, in agreement with the conclusion of Ref. 8. A comparison of the present theoretical results with the data of Ref. 8 shows agreement within error with the A_y data, but predicts A_{yy} values which are somewhat outside of the error bars. At 45°, for example, the measured value was -0.33 ± 0.12, while theory predicts a value of −0.135. This suggests that either the A_{yy} values of Ref. 8 have been overestimated by about 2σ, or that the energy dependence predicted by the theory is incorrect. Nevertheless, the evidence for a large *p*-wave contribution presented in Ref. 8 remains intact.

V. ASTROPHYSICAL *S* FACTOR AND CONCLUSIONS

The accepted value of the astrophysical *S* factor, when extrapolated to zero energy, is $S(0)=6.4\times10^{-6}$ keV b. This is based on the pure $E2$ semimicroscopic calculation [2], which fits the world data rather well at energies above

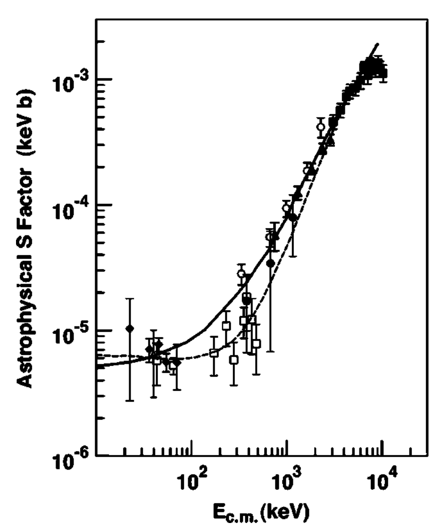

FIG. 3. The astrophysical *S*-factor energy dependence calculated using RRGM (solid line) presented along with world data for $^2\mathrm{H}(\vec{d},\gamma)^4\mathrm{He}$ absolute cross section measurements and the pure $E2$ semimicroscopic model calculation (dashed line) [2]. The data points are [22] (•), [23] (■), [24] (▲), [25] (◆), [26] (○), [27] (□), [6] (△).

$E_{\mathrm{c.m.}}=100$ keV. The present RRGM calculation also agrees with the higher energy data, and produces an S-factor curve which has a small positive slope, as opposed to the slightly negative slope for the pure $E2$ calculation. This positive slope is, of course, a result of the strong ($\approx$50%) p-wave contribution that has been confirmed by our experimental results. These results are illustrated in Fig. 3 along with the world data set. Note that the theoretical calculations are in absolute units and have not been normalized to the data.

The RRGM calculation was performed from 6 keV up to 9 MeV. When extrapolated to $E=0$, the value of the S factor is found to be $S(0)=4.8\times10^{-6}$ keV b, which is 25% lower than the previously accepted value. We therefore recommend that this lower value of $S(0)$ be adopted as the accepted value of the astrophysical S factor for the $^{2}\mathrm{H}(\vec{d},\gamma)^{4}\mathrm{He}$ reaction.

ACKNOWLEDGMENTS

The authors wish to acknowledge the help of the entire TUNL staff, and the continued support of the Director of TUNL, Dr. Werner Tornow. This work was partially supported by the U.S. Department of Energy under Grant Nos. DE-FG02-97ER41033 and DE-FG02-97ER41042.

[1] W. A. Fowler, G. R. Caughlan, and B. A. Zimmerman, Annu. Rev. Astron. Astrophys. **5**, 525 (1967).
[2] H. J. Assenbaum and K. Langanke, Phys. Rev. C **36**, 17 (1987).
[3] H. R. Weller, P. Colby, N. R. Roberson, and D. R. Tilley, Phys. Rev. Lett. **53**, 1325 (1984).
[4] S. Mellema, T. R. Wang, and W. Haeberli, Phys. Rev. C **34**, 2043 (1986).
[5] J. L. Langenbrunner, G. Feldman, H. R. Weller, D. R. Tilley, B. Wachter, T. Mertelmeier, and H. M. Hofmann, Phys. Rev. C **38**, 565 (1988).
[6] L. H. Kramer, Ph.D. thesis, Duke University, 1992.
[7] R. M. Whitton, H. R. Weller, E. Hayward, W. R. Dodge, and S. E. Kuhn, Phys. Rev. C **48**, 2355 (1993).
[8] L. H. Kramer, H. R. Weller, E. Hayward, R. M. Prior, and D. R. Tilley, Phys. Lett. B **304**, 208 (1993).
[9] H. R. Weller and N. R. Roberson, IEEE Trans. Nucl. Sci. **NC-28**, 1268 (1981).
[10] *Polarization Phenomena in Nuclear Reactions*, edited by H. H. Barschall (University of Wisconson Press, Madison, WI, 1971), p. xxv.
[11] M. J. Balbes, Ph.D. thesis, Duke University, 1992.
[12] R. G. Seyler and H. R. Weller, Phys. Rev. C **20**, 453 (1979).
[13] H. M. Hofmann, in *Proceedings of Models and Methods in Few-Body Physics, Lisboa, Portugal 1986*, edited by L. S. Ferreira, A. C. Fonseca, and L. Streit, Lecture Notes in Physics Vol. 273 (Springer, Berlin, 1987), p. 243.
[14] K. Wildermuth and Y. C. Tang, *A Unified Theory of the Nucleus* (Vieweg, Braunschweig, 1977).
[15] Y. C. Tang, *Topics in Nuclear Physics*, Lecture Notes in Physics Vol. 145 (Springer, Berlin, 1981).
[16] W. Kohn, Phys. Rev. **74**, 1763 (1948).
[17] R. B. Wiringa, V. G. J. Stokes, and R. Schiavilla, Phys. Rev. C **51**, 38 (1995).
[18] B. S. Pudliner, V. R. Pandharipande, S. C. P. J. Carlson, and R. B. Wiringa, Phys. Rev. C **56**, 1720 (1997).
[19] C. Winkler and H. M. Hofmann, Phys. Rev. C **55**, 684 (1997).
[20] A. Nogga, H. Kamada, and W. Glöckle, Phys. Rev. Lett. **85**, 944 (2000).
[21] T. Mertelmeier and H. M. Hofmann, Nucl. Phys. **A459**, 387 (1986).
[22] R. W. Zurmühle, W. E. Stephens, and H. H. Staub, Phys. Rev. **132**, 751 (1963).
[23] W. E. Meyerhof, W. Feldman, S. Gilbert, and W. O'Connell, Nucl. Phys. **A131**, 489 (1969).
[24] A. Degré, Ph.D. thesis, Université de Strasbourg, 1992.
[25] F. J. Wilkinson and F. E. Cecil, Phys. Rev. C **31**, 2036 (1985).
[26] H. R. Weller, P. Colby, J. L. Langenbrunner, Z. D. Huang, D. R. Tilley, F. D. Santos, A. Arriaga, and A. M. Eiro, Phys. Rev. C **34**, 32 (1986).
[27] C. A. Barnes *et al.*, Phys. Lett. B **197**, 315 (1987).